Published March 30, 2015, doi:10.4049/jimmunol.1400793

Epitope-Specific CD8$^+$ T Cell Kinetics Rather than Viral Variability Determine the Timing of Immune Escape in Simian Immunodeficiency Virus Infection

Alexey P. Martyushev,* Janka Petravic,* Andrew J. Grimm,* Hamid Alinejad-Rokny,* Shayarana L. Gooneratne,† Jeanette C. Reece,† Deborah Cromer,* Stephen J. Kent,† and Miles P. Davenport*

CD8$^+$ T cells are important for the control of chronic HIV infection. However, the virus rapidly acquires "escape mutations" that reduce CD8$^+$ T cell recognition and viral control. The timing of when immune escape occurs at a given epitope varies widely among patients and also among different epitopes within a patient. The strength of the CD8$^+$ T cell response, as well as mutation rates, patterns of particular amino acids undergoing escape, and growth rates of escape mutants, may affect when escape occurs. In this study, we analyze the epitope-specific CD8$^+$ T cells in 25 SIV-infected pigtail macaques responding to three SIV epitopes. Two epitopes showed a variable escape pattern and one had a highly monomorphic escape pattern. Despite very different patterns, immune escape occurs with a similar delay of on average 18 d after the epitope-specific CD8$^+$ T cells reach 0.5% of total CD8$^+$ T cells. We find that the most delayed escape occurs in one of the highly variable epitopes, and that this is associated with a delay in the epitope-specific CD8$^+$ T cells responding to this epitope. When we analyzed the kinetics of immune escape, we found that multiple escape mutants emerge simultaneously during the escape, implying that a diverse population of potential escape mutants is present during immune selection. Our results suggest that the conservation or variability of an epitope does not appear to affect the timing of immune escape in SIV. Instead, timing of escape is largely determined by the kinetics of epitope-specific CD8$^+$ T cells. ***The Journal of Immunology*****, 2015, 194: 000–000.**

The CD8$^+$ T cell response plays an important role in controlling chronic infection by HIV and SIV. These responses are elicited early in infection and help reduce viral loads in the acute phase of infection (1). However, many early CD8$^+$ T cell responses lose their ability to control virus because of viral "immune escape mutation," in which viral variants of an epitope emerge that are not recognized by the existing CD8$^+$ T cell response (2). Immune escape mutation often involves successive selection of mutants, both within a single epitope and across different epitopes over time. This can occur extremely rapidly in early infection, but it also continues throughout chronic infection, although the rate of selection is known to slow with time (3, 4). Several factors contribute to the timing of immune escape, including the magnitude and phenotype of the CD8$^+$ T cell response, as well as the ability of the virus to generate and tolerate mutations within the epitope (5).

The generation of the diversity of HIV quasispecies seen in an infected individual is a stochastic process involving both the underlying mutation rate (6, 7) and the variability of the epitope and the potential for a mutation to produce a viable escape mutation (8, 9). The subsequent selection of escape mutants depends on the replicative fitness of the escape mutant (10, 11), as well as the host environment, including both the strength of CD8$^+$ T cell immune pressure (4) and the availability of host CD4$^+$ T cells for infection (12). The dynamics of competition among strains during the course of infection are still not fully understood. Therefore, the timing and rate of appearance of one viral strain and its replacement by other strains tend to be unpredictable. The features commonly used to quantify escape dynamics are escape rate, time of escape, and the number of represented mutants in the sequences (3, 10, 13, 14). These parameters vary considerably from patient to patient and epitope to epitope, and also over time during the infection (4). A more refined understanding of why escape occurs when it does is needed and should ultimately assist in the design of better T cell–based vaccines and immunotherapies.

In the present study, we investigate the patterns of viral escape in SIV-infected pigtail macaques, using the results of deep sequencing of three CD8$^+$ T cell epitopes to study the frequency of different viral variants. Two of the three CTL epitopes show a high number of possible escape mutations, whereas one epitope has much more limited avenues of immune escape. The timing of immune escape appears independent of the inherent variability of the epitopes, and instead seems mainly determined by the kinetics of epitope-specific CD8$^+$ T cells to the epitope. An analysis of the escape variants demonstrates that multiple variants "audition for selection" at the peak of escape. The fact that so many mutants are present at the same time argues that they must be rapidly generated or already present within the viral pool at the time when immune pressure is applied. This suggests that the generation of CD8$^+$ T cell selection pressure rather than the generation of viable escape mutant virus is the major bottleneck to immune escape in HIV.

*Centre for Vascular Research, University of New South Wales, Sydney, New South Wales 2052, Australia; and †Department of Microbiology and Immunology, Peter Doherty Institute for Infection and Immunity, University of Melbourne, Parkville, Victoria 3010, Australia

Received for publication March 27, 2014. Accepted for publication March 1, 2015.

This work was supported by National Health and Medical Research Council (Australia) Grants 1025567 and 1052979. M.P.D. and S.J.K. are National Health and Medical Research Council (Australia) Research Fellows.

Address correspondence and reprint requests to Prof. Miles P. Davenport, Centre for Vascular Research, University of New South Wales, Sydney, NSW 2052, Australia. E-mail address: m.davenport@unsw.edu.au

The online version of this article contains supplemental material.

Materials and Methods

Ethics statement

Experiments on pigtail macaques (*Macaca nemestrina*) were approved by Commonwealth Scientific and Industrial Research Organization livestock industries Animal Ethics Committees (approval no. 1315) and cared for in accordance with Australian National Health and Medical Research Council guidelines.

Animals

We studied 25 Mane-A01*084$^+$ pigtail macaques (*M. nemestrina*) that have previously been described (15–19). Briefly, 17 of the animals were part of a vaccine trial of influenza-based vaccines, in which 7 macaques were controls (16), 5 received influenza viruses expressing the SIV Gag KP9 CD8$^+$ T cell epitope (17), and five received influenza viruses expressing KP9 and two CD8$^+$ T cell epitopes in Tat termed KSA10 and KVA10 (18). Eight pigtail macaques were enrolled in a therapeutic peptide-based vaccine trial (19) and received antiretroviral therapy (tenofovir and emtricitibine) from weeks 3 to 10 postinfection. Either no treatment (controls) or peptide-vaccine treatment (overlapping 15-mer Gag peptides only or overlapping 15-mer peptides from all nine SIV proteins) was given at weeks 4, 6, 8, and 10 postinfection. Supplemental Table I describes the treatments of the individual animals analyzed in the study. The Mane-A01*084$^+$ macaques (the restricting MHC class I allele for KP9, KVA10, and KSA10) were infected with SIV_{mac251}. Animals were anesthetized i.m. with ketamine (10 mg/kg) prior to any procedures. Postinfection plasma samples were taken first twice a week, then fortnightly, and later monthly (see Fig. 1A). As controls for the absence of immune pressure at the Mane-A01*084–restricted CTL epitopes KP9, KVA10, and KSA10, we also studied 28 Mane-A01*084$^-$ pigtail macaques. The Mane-A01*084$^-$ pigtail macaques were infected with SIV_{mac251} as part of the same studies as the Mane-A01*084$^+$ pigtail macaques (Supplemental Table II).

Characterization of epitope-specific CD8$^+$ T cells to three SIV epitopes

The kinetics of SIV-specific CD8 T cells to three SIV epitopes were measured by tetramer staining of CD3$^+$CD8$^+$ lymphocytes in fresh whole heparinized blood. The three epitopes all had the same MHC restriction, that is, Mane-A01*084. Mane-A01*084 tetrameric protein folded around either the KVA10 (SIV $Tat_{114–123}$), KSA10 (SIV $Tat_{87–96}$), or KP9 (SIV $Gag_{164–172}$) peptide epitope were used as previously described (17, 20). An example of the gating strategy for CD3$^+$CD8$^+$ lymphocytes staining for the three tetramers in a sample from one of the Mane-A01*084$^+$ pigtail macaques infected with SIV is shown in Fig. 1B.

These three CTL epitopes are restricted by the same MHC class I allele, Mane-A01*084, thus allowing us to select animals positive for this allele and study three epitopes at the same time in each animal. This substantially increased the strength of our study because we could observe similar patterns of early emergence of multiple variants at the start of escape in all three epitopes in the same animals. We have previously shown that the common escape motifs result in reduced T cell recognition (16, 21) and tetramers do not bind the escape mutant peptides well. No other Mane-A01*084–restricted SIV epitopes have been identified to date.

All tetramer staining data are available on the open source depository site (http://datadryad.org/resource/doi:10.5061/dryad.qn8n3) and upon request.

Pyrosequencing for escape at KP9, KVA10, and KSA10

To examine the effects of CD8$^+$ T cell selection on virus, we isolated and pyrosequenced plasma virus from serial time points after SIV infection as previously described (18, 22). Briefly, viral RNA from EDTA anticoagulated plasma was extracted using the QIAamp MinElute virus spin kit or QIAamp UltraSens RNA kit (Qiagen, Valencia, CA). Viral RNA was reverse transcribed and amplified using the SuperScript III One-Step RT-PCR system with Platinum Taq DNA Polymerase High Fidelity (Invitrogen, Carlsbad, CA) and MID-tagged primers (454; Sigma-Aldrich) spanning $Gag_{164–172}$ (KP9; KKFGAEVVP) and $Tat_{114–123}$ (KVA10; KKETVEKAVA) and $Tat_{87–96}$ (KSA10; KKAKANTSSA). The RT-PCR conditions were: 50˚C for 15 min; 94˚C for 2 min; 40 cycles of 94˚C for 15 s, 58˚C for 30 s, and 68˚C for 50 s; then 68˚C for 5 min. DNA from PCR products was purified by cutting out appropriate bands from a 1% agarose gel and using the QIAquick gel extraction kit (Qiagen). Amplicons were pooled at equimolar ratios and sequenced by the Australian Genome Research Facility using a Roche 454 system. Amino acid variation within the three epitopes (Gag KP9, Tat KVA10, and Tat KSA10) was examined using custom software written in BioRuby. Sequence reads that did not span the full amplicon or that contained ambiguous nucleotides were discarded to remove low quality sequences (23, 24). Reads were aligned against their respective reference sequences, and the portion of the read corresponding to the epitope was analyzed. Reads within the epitope that contained frameshift mutations were excluded, and the frequency of different amino acid sequences at each epitope was calculated. An example of the pattern of immune escape at KP9 by deep sequencing in one animal is shown in Fig. 1C.

*Epitope variability in Mane-A01*084$^-$ animals*

To assess variability across the Mane-A01*084 epitopes in the absence of CTL pressure at these sites, we sequenced plasma SIV RNA from 28 Mane-A01*084$^-$ animals 15–24 wk after SIV_{mac251} infection (Supplemental Table II; described in detail in Ref. 25). Briefly, the whole SIV_{mac251} genome was amplified in four overlapping fragments by RT-PCR using specifically designed primers from plasma cDNA. RT-PCR was performed in an Eppendorf realplex Mastercycler (Eppendorf, Hamburg, Germany) under the following conditions: 50˚C for 60 min; 94˚C for 2 min; 2 cycles of 94˚C for 15 s, 60˚C for 1 min, 68˚C for 4 min; 2 cycles of 94˚C for 15 s, 58˚C for 1 min, 68˚C for 4 min; 41 cycles of 94˚C for 15 s, 55˚C for 1 min, 68˚C for 4 min; 68˚C for 10 min. PCR products were run on a 0.7% agarose gel (Promega, Madison, WI) alongside a 1-kb DNA ladder (New England BioLabs, Ipswich, MA), the correct size bands were excised, and DNA was extracted using the QIAquick gel extraction kit (Qiagen).

Amplified plasma SIV cDNA concentrations were measured using the Qubit dsDNA HS assay kit and the Qubit 2.0 fluorometer (Life Technologies, Carlsbad, CA) and 4×10^8 copies from each of the four fragments were pooled to create a complete genome. Nextera XT DNA sample preparation kit (Illumina) was used to prepare libraries for sequencing. The libraries were sequenced in a MiSeq system (Illumina, San Diego, CA).

All sequencing data are available on the open source depository site (http://datadryad.org/resource/doi:10.5061/dryad.qn8n3) and upon request.

Measuring escape rate

To estimate the dynamics of viral replacement and compare the ability of SIV strains to survive and dominate under immune pressure, we define the escape rate (ER) as

$$ER(t_0, t_1) = g_{EM}(t_0, t_1) - g_{WT}(t_0, t_1), \quad (1)$$

where $g_{EM}(t_0,t_1)$ and $g_{WT}(t_0,t_1)$ are the growth rates of an escape mutant (EM) and a wild-type (WT), respectively, measured between time points t_0 and t_1.

We assume exponential growth/decay of EM and WT between two sequential measurements at time points t_0 and t_1, which amounts to linear interpolation between log-transformed data points (15, 26). The number of copies of WT and EM in plasma between t_0 and t_1 is given by the equations

$$WT(t_1) = WT(t_0)e^{g_{WT}(t_1 - t_0)} \quad (2)$$

$$EM(t_1) = EM(t_0)e^{g_{EM}(t_1 - t_0)} \quad (3)$$

The ER is defined as a difference in exponential growth rates of EM and WT and can then be found from

$$ER(t_0, t_1) = [\ln f_{EM}(t_1) - \ln f_{EM}(t_0) - \ln f_{WT}(t_1) + \ln f_{WT}(t_0)]/(t_1 - t_0) \quad (4)$$

where $f_{WT}(t)$ and $f_{EM}(t)$ are the fractions of WT and EM at time t, respectively (10, 12, 27).

The escape can be measured for two different strains, WT and EM, but in the case of the model of multiple variants there are many mutants that replace WT. Therefore, to measure total ER we use f_{WT} against $1 - f_{WT}$, but we can also measure individual ERs between WT and each mutant strain (WT, EM_i).

Estimating the time to 50% WT

If the percentage WT in the data changes from >50% at the time point t_1 to <50% at the subsequent time point t_2, we estimated the time to 50% WT between t_1 and t_2 using linear interpolation.

One animal (19351) at the KP9 epitope and three animals (19351, 26359, 8244) at the KSA10 epitope did not reach 50% WT by the last measurement, and we used linear extrapolation to estimate the time to 50% WT.

The number of new mutants appearing per day

Low levels of many sequence variants were often present as single copies in the sequencing data, likely due to sequencing error. The probability of

sequencing error is 10^{-4} per nucleotide. Because we are analyzing 27–30 bp epitopes, then the probability of at least one error in a sequence is $1 - (1–10^{-4})^{30} \approx 0.3\%$. To reduce the risk of including possible sequencing errors as mutants in our analysis, we used as a cut-off the threshold of 1% of total virus to analyze the appearance of new mutants. We defined the rate of appearance of new mutants, which we call the increase in mutants, as the number of new mutants appearing per day:

$$m'(t_i, t_{i+1}) = [m(t_{i+1}) - m(t_i)]/(t_{i+1} - t_i), \quad (5)$$

where $m(t_i)$ is the number of mutants at a frequency >1% in the sequence data at the time point t_i. The increase in mutants m' is discrete and takes values within time intervals defined by start and end time points t_i and t_{i+1}, respectively, that is, mutants with fraction <1% in the sequence were not taken into account in the values of $m(t_i)$ and $m(t_{i+1})$. For example, when the number of variants at >1% went from two to five in 3 d, this would be an average increase in variants of (5 mutants − 2 mutants)/3 d = 1 mutant per day.

Statistical analysis

Data analysis was performed using GraphPad Prism (version 6.01).

Results

Dynamics of epitope-specific CD8$^+$ T cells responding to SIV

Factors leading to the timing of CTL escape are imperfectly understood. We studied a pigtail macaque SIV infection model where three CTL epitopes are restricted by the same MHC class I allele in 25 macaques. We analyzed serial epitope-specific CD8$^+$ T cell numbers by MHC tetramer and immune escape by deep sequencing. The animals included in the study were collected from a variety of previous vaccination studies, and thus they varied in the initial magnitude of their CTL responses, as well as whether the response was a primary response (in control animals) or secondary response (in vaccinees) (see Supplemental Table I). We have previously studied the dynamics of immune escape at a well-characterized SIV Gag epitope, KP9 (4, 10). This epitope is recognized by CD8$^+$ T cells through the Mane-A01*084 allele (previously referred to as ManeA*10). These Mane-A01*084–restricted SIV-specific CD8$^+$ T cell responses arise within the first few weeks of infection. The magnitude of the CD8$^+$ T cell response declines after acute infection, in association with immune escape. Fig. 1D shows the kinetics of the epitope-specific KP9-specific CD8$^+$ T cells detected by tetramer analysis in serial blood samples from three representative macaques.

In addition to the KP9 immune response, we have also previously identified and characterized two additional Mane-A01*084–restricted CD8$^+$ T cell responses in SIV-infected pigtail macaques, the Tat KVA10 and Tat KSA10 epitopes (28) (Fig. 1D). As shown, the magnitude of immune response to the three epitopes differed across the animals, with some animals mounting a stronger response to Gag KP9, whereas some responded more strongly to either of the Tat epitopes KVA10 or KSA10. The appearance of immune escape variants by deep sequencing at the three epitopes is shown for three representative animals in Fig. 1E–G, showing that the frequency of the epitope-specific CD8$^+$ T cells changes over time coincidently with the rise and domination of epitope variants. Viral loads are shown in Fig. 1H.

The epitope-specific CD8$^+$ T cells to the three Mane-A01*084–restricted epitopes had quite different kinetics across the 25 macaques, with the KSA10 response peaking substantially later than the other two (Fig. 2A). The later peak of the KSA10-specific CD8$^+$ T cells could arise either because the response was initiated later, or because the response was slow growing. To better characterize the relationship between the appearance of CTLs and escape, we first analyzed the timing of the initial appearance of the epitope-specific CD8$^+$ T cells at the three epitopes (defined as the time when the CD8$^+$ T cell level appeared >0.01% of total CD8). By this criterion, all three responses arose at a similar time in early infection (Fig. 2B). We also investigated using a higher threshold for identifying the start of the response (for example 0.5% of total CD8$^+$ T cells, although other thresholds such as 1% produced essentially the same results). Using this higher threshold we observed a significant delay until the KSA10 response reached this level (Fig. 2C). When we directly estimated the growth rate of the epitope-specific CD8 T cell numbers to the different epitopes, we observed a significantly slower growth rate of the KSA10-specific CD8$^+$ T cells compared with the response to the other two epitopes (Fig. 2D).

Immune escape from CD8$^+$ T cell responses

The generation of CD8$^+$ T cell responses to an epitope is necessary to produce the immune selection pressure required to drive selection of escape mutant virus. However, it is also necessary that there are some viable viral mutants that both escape immune recognition and have sufficient replicative fitness to survive within the host. To study the frequency of different genotypes of the virus over time, we used pyrosequencing of plasma virus quasispecies at the three epitopes at serial time points (see Fig. 1C for an example). One way of characterizing the timing of immune escape is to analyze the time at which the frequency of the wild-type virus drops to 50% of the total viral load. Using this approach, we found that the timing of immune escape varied significantly among the three epitopes studied in a characteristic manner in the different animals (Fig. 2E). The KVA10 epitope usually escaped first (median, 23.22 d), followed by the KP9 epitope (median, 41.79 d) and the KSA10 epitope (median, 71.41 d).

Although the epitopes clearly escape at different times, it is not clear whether this is because of differences in the CD8$^+$ T cell responses or in the time taken for mutation and selection of the viral epitopes themselves.

Previous studies have suggested that the epitope variability or "entropy" may play a significant role in determining immune escape (9). To investigate the role of CD8$^+$ T cell response and viral variability, we used the same approach as in Liu et al. (9) to analyze the time from the detection of the CTL response to the time of 50% escape. Consistent with the differences in T cell kinetics described above, when we analyzed the time from first detection of the epitope-specific CD8$^+$ T cells to an epitope (at 0.01% of total CD8$^+$ T cells) until escape, we saw that escape appeared significantly delayed for the KSA10 epitope (Fig. 2F). However, when we used a higher threshold to define the start of the epitope-specific CD8$^+$ T cell response (0.5%), we found no significant variability between epitopes in the time from epitope-specific CD8$^+$ T cell numbers reaching 0.5% to time of escape (Fig. 2G) (the same was also true for other thresholds, such as 1%). The average time between epitope-specific CD8$^+$ T cells reaching 0.5% and viral escape reaching 50% wild-type was 17.93 ± 5.34 d.

A previous study has also suggested that the time to immune escape is negatively correlated with the number of the epitope-specific CD8$^+$ T cells measured early after infection (9). We also analyzed the relationship between the size of the CD8$^+$ T cell response and the time to escape for the different epitopes. We found a similar negative trend between CD8$^+$ T cell response magnitude and time to escape (although this was only significant for KP9, Fig. 3A–C). However, we also observed a trend for later peaks in the response to have lower magnitudes (Fig. 3D–F), thus significantly confounding the relationship between the magnitude of peak and the time of escape.

Variable patterns of CD8$^+$ T cell escape

In addition to the difference in timing of escape between the three epitopes, they also differ substantially in the patterns of escape

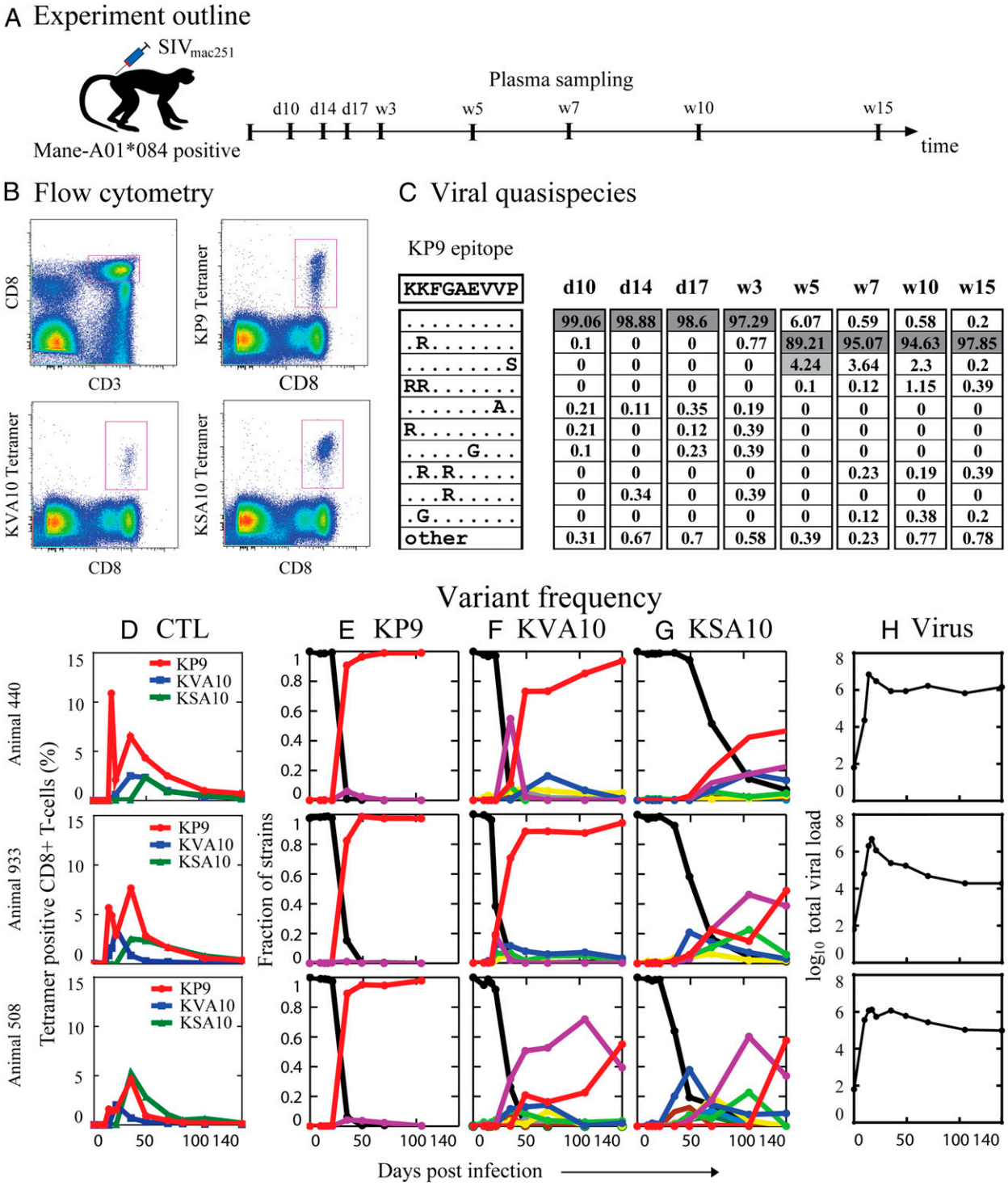

FIGURE 1. Summary of experimental approach. (**A**) SIV_{mac251} infection of pigtailed macaques and typical blood sampling intervals after infection. (**B**) Example of flow cytometric analysis of CTL responses in blood. $CD3^+CD8^+$ lymphocytes were stained with Mane-A01*084 tetramers folded around the KP9, KSA10, or KVA10 epitopes in animal 508. (**C**) Sample of analyzed plasma SIV sequences across the KP9 epitope over time after SIV infection in animal 508. The total number of sequences for different days was between 500 and 1000, and the numbers represent percentages of total. (**D**) Examples of the frequency of epitope-specific $CD8^+$ T cells to three epitopes in three animals over time after SIV infection. (**E**–**G**) Examples of frequencies of epitope variants in three animals. Black line represents wild-type and colored lines represent frequencies of different strains >1%. (**H**) Total viral load over time in three animals.

mutant strains observed. The KP9 epitope characteristically escapes through a lysine to arginine mutation at position 165 of the Gag protein (K165R mutation), and this mutant completely replaced the wild-type virus in 21 of 25 animals. Replacement of wild-type virus by an alternative mutation (P172S) is also seen in a much smaller proportion (3 of 25) of animals. One animal (517) did not escape at KP9. The two Tat epitopes show a much broader diversity of observed escape mutations, with different animals developing different escape mutations, and multiple variants present within each animal. Unlike the KP9 epitope, where one variant rapidly progressed to fixation, the frequency of individual mutants at the KSA10 and KVA10 epitopes fluctuated over time, with waves of different mutants dominating for a time and then declining in frequency (shown in the examples in Fig. 1F and 1G).

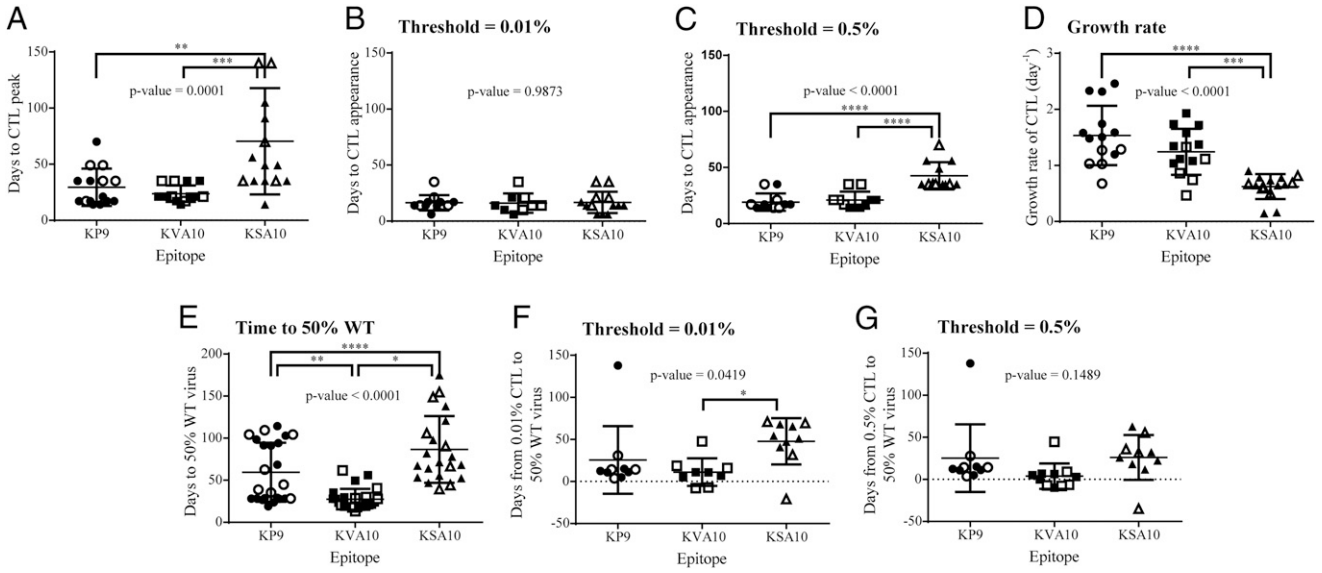

FIGURE 2. Differences in timing of epitope-specific CD8$^+$ T cells and escape across epitopes (statistics using one-way ANOVA with multiple comparisons posttest). (**A**) Time to peak epitope-specific CD8$^+$ T cells is significantly longer for KSA10 epitope. (**B**) There is no difference across epitopes in the time in which CD8$^+$ T cells specific for each epitope reached 0.01% of total CD8 T cells. (**C**) CD8$^+$ T cells specific to KSA10 epitope take significantly longer time to reach 0.5% of the total. (**D**) Growth rate of CD8$^+$ T cells specific to KSA10 is significantly slower than the growth rates of CD8s specific to the other epitopes. (**E**) Time from challenge to 50% wild-type differs significantly across epitopes: KVA10 on average escapes first, followed by KP9 and finally by KSA10. (**F**) Time from epitope-specific CD8$^+$ T cells reaching 0.01% of total to viral population reaching 50% of wild-type in plasma is significantly longer for KSA10. (**G**) Time from epitope-specific CD8s reaching 0.5% of total to viral population reaching 50% wild-type in plasma does not differ significantly across epitopes. In all panels, solid symbols represent control animals and open symbols represent vaccinated animals.

To compare the diversity of mutations seen in the three epitopes, we analyzed the number of different mutations that were seen across all the different animals. To avoid counting potential sequencing errors, we counted only strains that were present at >1% of the total sequences at a given time point. This showed the remarkably small number of escape mutant strains seen at KP9, with the dominant K165R mutation seen at >1% in 24 of 25 animals and the P172S mutant seen at >1% in 13 of 25 animals. However, other than these mutations, only one other mutation was seen in >20% of animals, and only 20 different mutants ever achieved a frequency of >1% in any animal at any time point (Fig. 4A). The diversity of mutants at the KVA10 and KSA10 epitopes was much higher by comparison. Both epitopes had mutations seen in all animals (two for KVA10, one for KSA10). Similarly, KVA10 had a total of 18 mutations present in >20% of animals and a total of 98 mutations seen overall (Fig. 4B). KSA10 had 16 mutations present in >20% of animals and 93 mutations seen overall (Fig. 4C). Thus, it appears that there is much more variability in

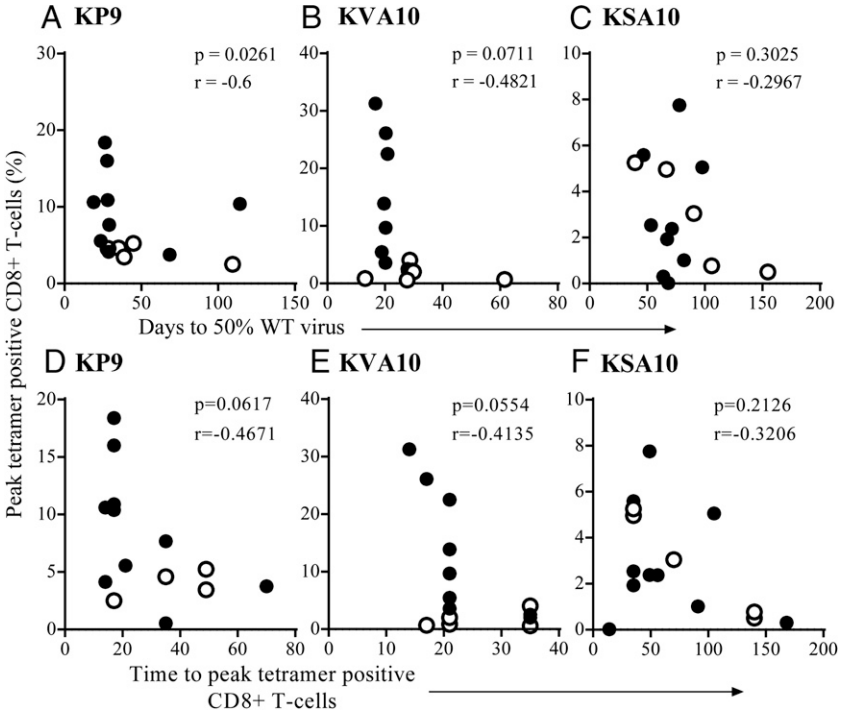

FIGURE 3. The association between the epitope-specific CD8$^+$ T cell response magnitude and time to escape suggests that higher response leads to earlier escape (**A**–**C**) [only significant for KP9 (A), by Spearman correlation]. However, the epitope-specific CD8$^+$ T cell response magnitude is also associated with time to peak of tetramer$^+$CD8$^+$ T cells (**D**–**F**) (although this is not significant), confounding the analysis. In all panels, solid symbols represent control animals and open symbols represent vaccinated animals.

the KVA10 and KSA10 epitopes than in the KP9 epitope, even though it is the KSA10 epitope that escapes slowly. This is somewhat surprising given that the KP9 epitope escapes with a similar delay as for the highly variable KSA10 epitope, measured from the time $CD8^+$ T cell response reaching 0.5% to when escape is observed.

*Variability of SIV epitopes in Mane-A01*084$^-$ animals*

The restricted pattern of escape at the KP9 epitope may have arisen because of a very conserved protein structure at this epitope, limiting the mutations that would be tolerated, or because the T cell repertoire responding to KP9 was sufficiently promiscuous to cross-recognize many of the alternative possible mutations (29). To understand the inherent variability of the epitope, we analyzed the sequence evolution of these epitopes in 28 Mane-A01*084$^-$ animals that had been infected with the same SIV_{mac251} virus stock (Supplemental Table II) as controls. The viral sequences from these animals were examined using Illumina sequencing from plasma virus obtained in chronic infection. We did not see any common escape mutations in any of the 28 Mane-A01*084$^-$ animals. Comparing the number of unique mutations observed at >1% of the viral sequences in any animal, we found only one amino acid mutation and five silent nucleotide mutations at the highly conserved KP9 epitope (Fig. 4D). Consistent with the variability in Mane-A01*084$^+$ animals, we found a much higher number of variants at the other epitopes. We found six amino acid plus five silent nucleotide mutations in the KVA10, and eight amino acid plus one silent nucleotide change at the KSA10 epitope. In summary, there was minimal variation across all three epitopes, although the variation was slightly higher in KVA10 and KSA10 (Fig. 4D). This higher level of amino acid mutations suggests that even in Mane-A01*084$^-$ animals the KVA10 and KSA10 epitopes are able to tolerate a wider variety of mutations than does the KP9 epitope.

Rapid but transient emergence of multiple mutants

The analysis above demonstrates the wide variety of mutants that were observed in the different animals, particularly for the KVA10 and KSA10 epitopes. However, it is not clear whether this wide variety of mutants arose owing to a slow rate of generation of mutants during a long period of chronic infection, or whether these mutations are rapidly produced during infection. The highly restricted and stereotyped nature of immune escape at the KP9 epitope may suggest that perhaps individual animals adopted a particular escape mutation (K165R in 21 of 25 animals or P172S in 3 of 25 animals) simply because this was the only mutation that arose in these animals. However, our pyrosequencing data showed presence of the minor P172S mutant at low frequency, even in animals where K165R eventually dominated. Thus, the P172S mutation was seen in 18 of 25 animals at some time during infection and dominated at the last time point in 3 of these. However, in 11 of 18 animals in which the P172S mutation was present at >1%, the frequency of the P172S mutation peaked in frequency right at the peak of escape (just after the time when the wild-type strain dropped to 50% in the sample, Fig. 1E). That is, even in animals in which the K165R mutation was rapidly replacing wild-type virus, the P172S mutation was present right at the peak of escape. Using a permutation approach, we found that the co-occurrence of these two events in 11 of 18 animals is extremely unlikely by chance ($p < 10^{-5}$), showing that the timing of co-occurrence of the K165R and P172S mutations is closely aligned.

In addition to the K165R and P172S mutations at KP9, there were also several other minor mutants observed. To analyze the dynamics of these minor variants during immune escape, we looked at the number of variants present at >1% of the total virus in three stages of escape: 1) pre-escape, a time interval before escape when the fraction of wild-type virus was >90%; 2) escape, a time interval when wild-type virus is <90% but >1%; and 3) post-escape, a time interval after escape when the fraction of wild-type becomes <1% (disappears in terms of our chosen threshold). Fig. 5A shows that the number of KP9 epitope variants observed in the viral quasispecies peaked right in the middle of escape.

We also investigated whether the "burst" of different mutants observed at the peak of escape in KP9 was also seen in the other two epitopes. Both the KVA10 and KSA10 Tat epitopes showed a transient rapid expansion in the number of epitope variants observed just around the time of escape (Fig. 5B, 5C), decreasing in the post-escape period (as one escape mutant became dominant). Taken together, these results demonstrate that immune escape does not occur as a simple process of individual mutations arising slowly and sequentially over time. Instead, the coordinated emergence of multiple escape variants during the peak of escape suggests that these variants must have been present in the viral quasispecies at around the same time and selected together by the epitope-specific $CD8^+$ T cell response.

The fact that multiple mutants were seen at the peak of the response suggests strongly that the variants must have been present in a narrow window of time to be selected together. However,

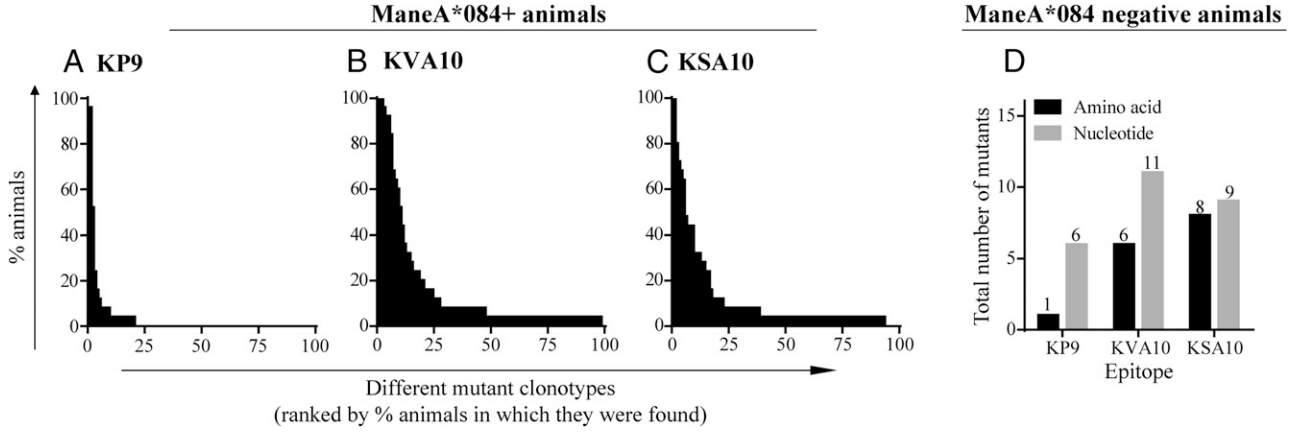

FIGURE 4. Variability of epitopes measured by the percentage of animals sharing the same mutant strains. (**A**–**C**) All strains observed at >1% at any time at (A) KP9, (B) KVA10, and (C) KSA10 in all ManeA01*084$^+$ animals were listed, with the *x*-axis representing the rank order on the list and the *y*-axis representing the percentage of animals sharing this strain. (**D**) Total number of strains observed >1% at any time at the three epitopes in all the ManeA01*084$^-$ animals.

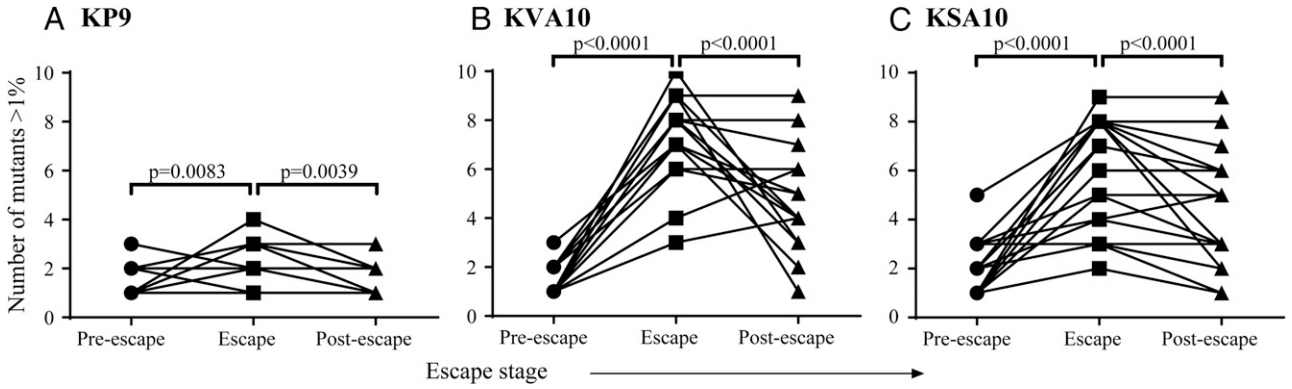

FIGURE 5. Many mutants arise around the time of escape. The number of mutants at a given epitope that are present at >1% are shown at different times relative to the time of immune escape for the Gag KP9 (**A**), Tat KVA10 (**B**), and KSA10 epitopes (**C**). Pre-escape is the period during which the percentage wild-type was >90%; escape is the period with the percentage wild-type between 90 and 1%; and post-escape is the period with the percentage wild-type lower <1%. In (A), the data for a large proportion of animals coincide.

because the immune pressure may have been present for some time before we observe escape, it is in principle possible that this gives time for a number of different mutants to be produced slowly and sequentially over time, rather than them being already present (or produced in rapid succession) in the viral quasispecies. Thus, we might speculate that if viral mutants are produced slowly over time, then the longer it takes to escape, the more mutants we expect to arise during the time of escape selection, and thus should be seen in our study. Therefore, we might predict that the number of mutants observed would increase when the rate of escape was slower, as slow escape would give more time for mutants to arise. Alternatively, if mutants are already present, then we might expect that the rate of emergence of mutants would be positively correlated with the overall escape rate, because faster selection gives less replication cycles in which to select for only the "fittest" virus. The latter appears to be the case, as the rate of immune escape (suppression of wild-type virus) is positively correlated with the peak rate of increase in the number of mutants (Fig. 6). The KP9 epitope shows the trend of increase in the peak number of new mutants with the increase in the escape rate, but because of the small number of mutant strains present (one or two) the noise in the data prevents it from reaching significance. In the more variable Tat epitopes KVA10 and KSA10 the correlation was highly significant. These results demonstrate that a wide variety of mutants can be selected very rapidly, and thus must either preexist in the viral quasispecies or emerge extremely rapidly during infection.

Discussion

For immune escape to be observed, a number of events must occur. First, there must be a sufficient level of immune pressure on the wild-type sequence so that an escape mutant can enjoy a selective advantage. However, the benefits of reduced immune recognition are often counterbalanced by a "fitness cost" of the escape mutation, because of reduced replicative fitness (10). The net selective advantage of escape will be the balance of this reduced recognition and reduced replicative fitness. Thus, the number of potentially viable escape mutations at a given epitope will be constrained by both viral and immune factors. On the viral side, epitopes in a highly conserved region of the virus may pay a high fitness cost of mutation, meaning that only a few mutations are potentially viable. On the immune side, the T cell response may cross-recognize some potential escape mutants, reducing their selective advantage (29). Therefore, the number of possible escape mutants may vary considerably between epitopes. Additionally, the probability of generating any given amino acid variant through mutation may also vary, depending on the underlying gene sequence.

The different steps in immune escape discussed above contribute to a high variability in the timing of immune escape between individuals in both HIV and SIV infection. This is most likely driven by one of two possible mechanisms, that is, either 1) delayed escape may be the result of the time taken for immune and other selective pressures to arise and select out appropriate variants, or 2) delayed escape may be a result of the time taken for the initial escape mutation to arise in the viral population (Fig. 7). In the former case, the kinetics of the immune response will be the major determinant of when immune escape will occur. In the latter case, the inherent conservation or variability of the viral sequence at an epitope will determine when escape occurs. Through our detailed study of immune escape across three epitopes that differ widely in their variability in 25 SIV-infected macaques we found that, once the kinetics of the immune response have been taken into account, escape occurs with similar delay after the appearance of immune response. Specifically, after the epitope-specific $CD8^+$ T cell numbers reached a threshold close to 0.5% of total $CD8^+$ T cells, escape followed after on average 18 d. This delay did not appear to be strongly affected by whether the animals had been previously vaccinated (and thus whether the response was a primary or secondary response), because similar delays were observed in previously vaccinated and unvaccinated animals (Fig. 2).

The escape rates reported for HIV are usually much slower than in SIV (30, 31). The reason for slower observed escape may be because of late diagnosis in most cases (as escape rates slow down in time) (4) and infrequent sampling. Indeed, when escape is detected very early in HIV infection and with more frequent sampling, the observed escape rates (3) are closer to those seen in SIV infection of macaques (10). The impact of epitope variability on the timing of immune escape has also been investigated in HIV (9, 32). There are a number of clear differences between these studies of HIV and our studies of SIV. SIV allows challenge with a standard stock of virus, and thus escape mutation occurred on a similar viral backbone in the different animals (notwithstanding recent mutations occurring after challenge). Additionally, we studied escape at three epitopes restricted through the same MHC class I allele, which further reduces variability within the system. This allowed us to observe the broad diversity of escape patterns at individual epitopes, occurring on the same viral backbone, across a large number of animals. Our quantification of the underlying variability of the epitopes (in the absence of immune

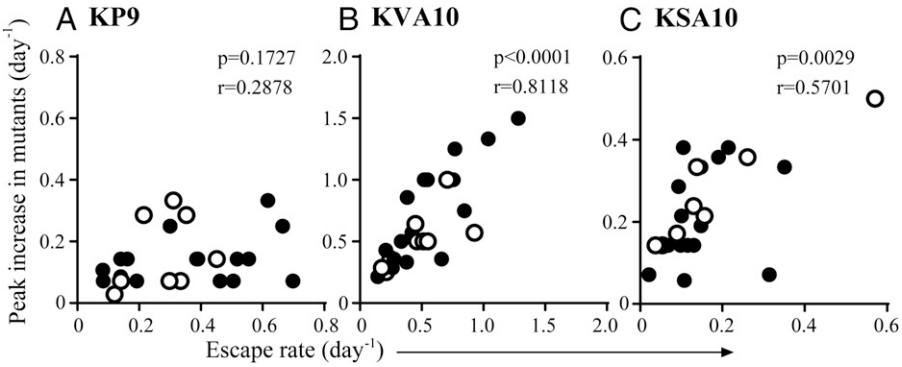

FIGURE 6. The peak increase in the number of new mutants is positively correlated with maximum escape rate. (**A**) For KP9 there is a positive trend. (**B** and **C**) For KVA10 (B) and for KSA10 (C) the correlation is highly significant (Spearman correlation). In all panels, solid symbols represent control animals and open symbols represent vaccinated animals.

recognition) also differed. We analyzed the degree of mutation seen in the epitope in animals infected with the same virus but lacking the appropriate MHC. In contrast, epitope variability in humans is usually determined by reference to the number of variants seen in the HIV sequence database, which contains often consensus sequences from a very diverse population of hosts and viruses. Finally, our definition of time to escape also differed. We aimed to separate the timing of the immune response from the delay from immune response to escape. Thus, we measured time from the epitope-specific $CD8^+$ T cell response reaching 0.5% until escape.

Previous studies of the emergence of drug-resistant mutations (33–37) and immune escape mutations (38) have speculated on the question of "pre-existence" of drug resistance, that is, whether drug-resistant mutants exist in the viral population before treatment or arise during the course of therapy (35–37). In principle, one could sequence all viral mutants to find the frequency of different point mutations prior to therapy (and indeed one would expect to find a very large number of variants owing to the high error rate of viral reverse transcriptase). However, in practice the frequency of sequencing error may exceed the frequency of the mutants themselves in vivo (39). Therefore, we require alternative methods of determining pre-existence of minor variants. Our approach of identifying the temporal emergence of multiple minor mutants during immune escape demonstrates not only that minor mutants are present, but that they are also selected during immune escape. The fact that so many minor epitope mutants are present may indeed not be surprising. The large population size of HIV within the infected individual and the high mutation rate of HIV and SIV mean that many single point mutants are present at very low levels. However, previous studies have suggested that the entropy of an epitope may determine the timing of escape (9, 40), and there is some debate over whether the census population size (number of virions in the host) or the effective population size of HIV is the more appropriate population to consider when estimating the diversity of variation expected (as reviewed in Ref. 41).

Our studies show that, at the time of initial escape, there are a variety of different potential mutants vying for dominance. The fact that these multiple variants are observed synchronously is not consistent with delayed escape being due to the long time until the initial generation of escape mutation. It suggests that multiple escape variants were all simultaneously present or rapidly generated during the period of selection for escape. Additionally, our work demonstrates that the time between immune response and viral escape does not differ significantly between a highly constrained epitope (KP9) and much more variable epitopes (KSA10 and KVA10) (Figs. 2, 4). Taken together, these results suggest that rapid escape occurs regardless of the degree of conservation of the viral sequence, likely because mutants are generated so rapidly in SIV.

Viral escape from $CD8^+$ T cell immune responses poses a significant challenge for the development of T cell–based vaccines. If viral mutation can simply avoid vaccine-induced responses, this may lead to loss of immune control of virus in an individual host, and potentially the spread of vaccine-resistant virus in the population. One solution to this is the targeting of highly conserved epitopes, where the virus is relatively constrained. The KP9 epitope would appear ideal from this perspective, as we observe only a few possible escape variants seen in animals responding to this epitope, and very little variability among nonresponder animals

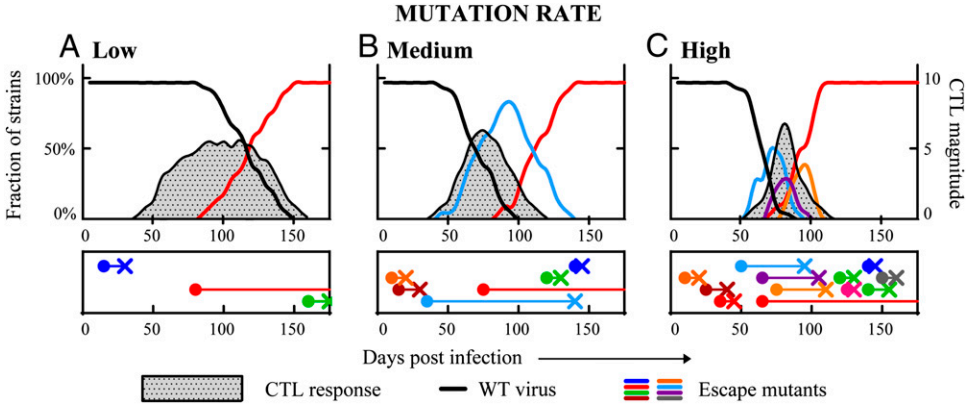

FIGURE 7. Influence of immune pressure and mutation rate on the timing of escape. (**A**) When the viral mutation rate is low, $CD8^+$ T cell immune pressure (shaded area) specific for the wild-type virus (black line) must persist for some time before a suitable mutant strain (colored lines) arises, leading to escape. Thus, there is a delay between the $CD8^+$ T cell response and immune escape. (**B** and **C**) For higher mutation rates, multiple viral mutants arise regularly, so there is little delay "waiting" for a mutation event.

(Fig. 4A). However, despite this apparent sequence conservation, the KP9 epitope escapes early in infection, and we have previously demonstrated that vaccination can lead to even earlier escape (4).

An alternative method for identifying vaccine epitopes might be to identify epitopes that escape late, on the basis that delayed escape might indicate that it was difficult for the virus to avoid immune recognition. In our study, escape at the KSA10 epitope was significantly delayed compared with the other two epitopes. However, this did not appear driven by restrictions on viral variability at this epitope, as the KSA10 epitope was highly variable (Fig. 4C). Instead, it seems that the delayed escape was due to the long time taken for the maturation of the KSA10-specific $CD8^+$ T cell response (Fig. 2C, 2D). Once the KSA10 response was established, the time between the epitope-specific $CD8^+$ T cell responses reaching 0.5% of total $CD8^+$ T cells and the time of 50% escape was very similar between the different epitopes (Fig. 2G). Because vaccination aims to drive an earlier and stronger $CD8^+$ T cell response, it seems possible that this would simply drive even earlier immune escape, as we have found with previous studies utilizing vaccines including a limited number of CTL epitopes (17, 18).

In summary, in this study of 25 macaques across three separate SIV-specific $CD8^+$ T cell epitopes, we found that the timing of immune escape was temporally and predictably related to the appearance of the epitope-specific $CD8^+$ T cell response, occurring ~18 d after. Furthermore, we found that the nature of the very initial escape mutations observed, with multiple viral quasispecies emerging coincidently with the appearance of the epitope-specific response, strongly suggests that a number of possible escape mutants must either pre-exist in the viral quasispecies or emerge extremely rapidly during infection. An improved understanding of factors that govern immune escape should enhance efforts to control HIV-1 replication through T cell immunity.

Disclosures

The authors have no financial conflicts of interest.

References

1. Schmitz, J. E., M. J. Kuroda, S. Santra, V. G. Sasseville, M. A. Simon, M. A. Lifton, P. Racz, K. Tenner-Racz, M. Dalesandro, B. J. Scallon, et al. 1999. Control of viremia in simian immunodeficiency virus infection by $CD8^+$ lymphocytes. *Science* 283: 857–860.
2. Carlson, J. M., J. Listgarten, N. Pfeifer, V. Tan, C. Kadie, B. D. Walker, T. Ndung'u, R. Shapiro, J. Frater, Z. L. Brumme, et al. 2012. Widespread impact of HLA restriction on immune control and escape pathways of HIV-1. *J. Virol.* 86: 5230–5243.
3. Goonetilleke, N., M. K. P. Liu, J. F. Salazar-Gonzalez, G. Ferrari, E. Giorgi, V. V. Ganusov, B. F. Keele, G. H. Learn, E. L. Turnbull, M. G. Salazar, et al. 2009. The first T cell response to transmitted/founder virus contributes to the control of acute viremia in HIV-1 infection. *J. Exp. Med.* 206: 1253–1272.
4. Loh, L., J. Petravic, C. J. Batten, M. P. Davenport, and S. J. Kent. 2008. Vaccination and timing influence SIV immune escape viral dynamics in vivo. *PLoS Pathog.* 4: e12.
5. Martínez-Picado, J., J. G. Prado, E. E. Fry, K. Pfafferott, A. Leslie, S. Chetty, C. Thobakgale, I. Honeyborne, H. Crawford, P. Matthews, et al. 2006. Fitness cost of escape mutations in p24 Gag in association with control of human immunodeficiency virus type 1. *J. Virol.* 80: 3617–3623.
6. Mansky, L. M., and H. M. Temin. 1995. Lower in vivo mutation rate of human immunodeficiency virus type 1 than that predicted from the fidelity of purified reverse transcriptase. *J. Virol.* 69: 5087–5094.
7. Nowak, M. 1990. HIV mutation rate. *Nature* 347: 522.
8. Ferrari, G., B. Korber, N. Goonetilleke, M. K. P. Liu, E. L. Turnbull, J. F. Salazar-Gonzalez, N. Hawkins, S. Self, S. Watson, M. R. Betts, et al. 2011. Relationship between functional profile of HIV-1 specific CD8 T cells and epitope variability with the selection of escape mutants in acute HIV-1 infection. *PLoS Pathog.* 7: e1001273.
9. Liu, M. K. P., N. Hawkins, A. J. Ritchie, V. V. Ganusov, V. Whale, S. Brackenridge, H. Li, J. W. Pavlicek, F. Cai, M. Rose-Abrahams, et al. 2013. Vertical T cell immunodominance and epitope entropy determine HIV-1 escape. *J. Clin. Invest.* 123: 380–393.
10. Fernandez, C. S., I. Stratov, R. De Rose, K. Walsh, C. J. Dale, M. Z. Smith, M. B. Agy, S.-L. Hu, K. Krebs, D. I. Watkins, et al. 2005. Rapid viral escape at an immunodominant simian-human immunodeficiency virus cytotoxic T-lymphocyte epitope exacts a dramatic fitness cost. *J. Virol.* 79: 5721–5731.
11. Friedrich, T. C., E. J. Dodds, L. J. Yant, L. Vojnov, R. Rudersdorf, C. Cullen, D. T. Evans, R. C. Desrosiers, B. R. Mothé, J. Sidney, et al. 2004. Reversion of CTL escape-variant immunodeficiency viruses in vivo. *Nat. Med.* 10: 275–281.
12. Petravic, J., L. Loh, S. J. Kent, and M. P. Davenport. 2008. $CD4^+$ target cell availability determines the dynamics of immune escape and reversion in vivo. *J. Virol.* 82: 4091–4101.
13. Asquith, B., Y. Zhang, A. J. Mosley, C. M. de Lara, D. L. Wallace, A. Worth, L. Kaftantzi, K. Meekings, G. E. Griffin, Y. Tanaka, et al. 2007. In vivo T lymphocyte dynamics in humans and the impact of human T-lymphotropic virus 1 infection. *Proc. Natl. Acad. Sci. USA* 104: 8035–8040.
14. Fischer, W., V. V. Ganusov, E. E. Giorgi, P. T. Hraber, B. F. Keele, T. Leitner, C. S. Han, C. D. Gleasner, L. Green, C.-C. Lo, et al. 2010. Transmission of single HIV-1 genomes and dynamics of early immune escape revealed by ultra-deep sequencing. *PLoS ONE* 5: e12303.
15. Reece, J., J. Petravic, M. Balamurali, L. Loh, S. Gooneratne, R. De Rose, S. J. Kent, and M. P. Davenport. 2012. An "escape clock" for estimating the turnover of SIV DNA in resting $CD4^+$ T cells. *PLoS Pathog.* 8: e1002615.
16. Smith, M. Z., C. J. Dale, R. De Rose, I. Stratov, C. S. Fernandez, A. G. Brooks, J. Weinfurter, K. Krebs, C. Riek, D. I. Watkins, et al. 2005. Analysis of pigtail macaque major histocompatibility complex class I molecules presenting immunodominant simian immunodeficiency virus epitopes. *J. Virol.* 79: 684–695.
17. Sexton, A., R. De Rose, J. C. Reece, S. Alcantara, L. Loh, J. M. Moffat, K. Laurie, A. Hurt, P. C. Doherty, S. J. Turner, et al. 2009. Evaluation of recombinant influenza virus-simian immunodeficiency virus vaccines in macaques. *J. Virol.* 83: 7619–7628.
18. Reece, J. C., S. Alcantara, S. Gooneratne, S. Jegaskanda, T. Amaresena, C. S. Fernandez, K. Laurie, A. Hurt, S. L. O'Connor, M. Harris, et al. 2013. Trivalent live attenuated influenza-simian immunodeficiency virus vaccines: efficacy and evolution of cytotoxic T lymphocyte escape in macaques. *J. Virol.* 87: 4146–4160.
19. De Rose, R., C. S. Fernandez, M. Z. Smith, C. J. Batten, S. Alcântara, V. Peut, E. Rollman, L. Loh, R. D. Mason, K. Wilson, et al. 2008. Control of viremia and prevention of AIDS following immunotherapy of SIV-infected macaques with peptide-pulsed blood. *PLoS Pathog.* 4: e1000055.
20. De Rose, R., R. D. Mason, L. Loh, V. Peut, M. Z. Smith, C. S. Fernandez, S. Alcantara, T. Amarasena, J. Reece, N. Seddiki, et al. 2008. Safety, immunogenicity and efficacy of peptide-pulsed cellular immunotherapy in macaques. *J. Med. Primatol.* 37(Suppl. 2): 69–78.
21. Mason, R. D., S. Alcantara, V. Peut, L. Loh, J. D. Lifson, R. De Rose, and S. J. Kent. 2009. Inactivated simian immunodeficiency virus-pulsed autologous fresh blood cells as an immunotherapy strategy. *J. Virol.* 83: 1501–1510.
22. Burwitz, B. J., J. B. Sacha, J. S. Reed, L. P. Newman, F. A. Norante, B. N. Bimber, N. A. Wilson, D. I. Watkins, and D. H. O'Connor. 2011. Pyrosequencing reveals restricted patterns of $CD8^+$ T cell escape-associated compensatory mutations in simian immunodeficiency virus. *J. Virol.* 85: 13088–13096.
23. Smyth, R. P., T. E. Schlub, A. J. Grimm, C. Waugh, P. Ellenberg, A. Chopra, S. Mallal, D. Cromer, J. Mak, and M. P. Davenport. 2014. Identifying recombination hot spots in the HIV-1 genome. *J. Virol.* 88: 2891–2902.
24. Schlub, T. E., A. J. Grimm, R. P. Smyth, D. Cromer, A. Chopra, S. Mallal, V. Venturi, C. Waugh, J. Mak, and M. P. Davenport. 2014. Fifteen to twenty percent of HIV substitution mutations are associated with recombination. *J. Virol.* 88: 3837–3849.
25. Gooneratne, S., H. Alinejad-Rokny, D. Ebrahimi, P. S. Bohn, R. W. Wiseman, D. H. O'Connor, M. P. Davenport, and S. J. Kent. 2014. Linking pig-tailed macaque major histocompatibility complex class I haplotypes and cytotoxic T lymphocyte escape mutations in SIV infection. *J. Virol.* 88: 14310–14325.
26. Davenport, M. P., R. M. Ribeiro, and A. S. Perelson. 2004. Kinetics of virus-specific $CD8^+$ T cells and the control of human immunodeficiency virus infection. *J. Virol.* 78: 10096–10103.
27. Balamurali, M., J. Petravic, L. Loh, S. Alcantara, S. J. Kent, and M. P. Davenport. 2010. Does cytolysis by $CD8^+$ T cells drive immune escape in HIV infection? *J. Immunol.* 185: 5093–5101.
28. Mason, R. D., R. De Rose, and S. J. Kent. 2009. Differential patterns of immune escape at Tat-specific cytotoxic T cell epitopes in pigtail macaques. *Virology* 388: 315–323.
29. Davenport, M. P., D. A. Price, and A. J. McMichael. 2007. The T cell repertoire in infection and vaccination: implications for control of persistent viruses. *Curr. Opin. Immunol.* 19: 294–300.
30. Ganusov, V. V., N. Goonetilleke, M. K. P. Liu, G. Ferrari, G. M. Shaw, A. J. McMichael, P. Borrow, B. T. Korber, and A. S. Perelson. 2011. Fitness costs and diversity of the cytotoxic T lymphocyte (CTL) response determine the rate of CTL escape during acute and chronic phases of HIV infection. *J. Virol.* 85: 10518–10528.
31. Asquith, B., C. T. T. Edwards, M. Lipsitch, and A. R. McLean. 2006. Inefficient cytotoxic T lymphocyte-mediated killing of HIV-1-infected cells in vivo. *PLoS Biol.* 4: e90.
32. Ferguson, A. L., J. K. Mann, S. Omarjee, T. Ndung'u, B. D. Walker, and A. K. Chakraborty. 2013. Translating HIV sequences into quantitative fitness landscapes predicts viral vulnerabilities for rational immunogen design. *Immunity* 38: 606–617.
33. Metzner, K. J., A. U. Scherrer, B. Preiswerk, B. Joos, V. von Wyl, C. Leemann, P. Rieder, D. Braun, C. Grube, H. Kuster, et al. 2013. Origin of minority drug-

resistant HIV-1 variants in primary HIV-1 infection. *J. Infect. Dis.* 208: 1102–1112.
34. Paredes, R., C. M. Lalama, H. J. Ribaudo, B. R. Schackman, C. Shikuma, F. Giguel, W. A. Meyer, III, V. A. Johnson, S. A. Fiscus, R. T. D'Aquila, et al. 2010. Pre-existing minority drug-resistant HIV-1 variants, adherence, and risk of antiretroviral treatment failure. *J. Infect. Dis.* 201: 662–671.
35. Ribeiro, R. M., S. Bonhoeffer, and M. A. Nowak. 1998. The frequency of resistant mutant virus before antiviral therapy. *AIDS* 12: 461–465.
36. Ribeiro, R. M., and S. Bonhoeffer. 2000. Production of resistant HIV mutants during antiretroviral therapy. *Proc. Natl. Acad. Sci. USA* 97: 7681–7686.
37. Alexander, H. K., and S. Bonhoeffer. 2012. Pre-existence and emergence of drug resistance in a generalized model of intra-host viral dynamics. *Epidemics* 4: 187–202.
38. Liu, Y., J. I. Mullins, and J. E. Mittler. 2006. Waiting times for the appearance of cytotoxic T-lymphocyte escape mutants in chronic HIV-1 infection. *Virology* 347: 140–146.
39. Henn, M. R., C. L. Boutwell, P. Charlebois, N. J. Lennon, K. A. Power, A. R. Macalalad, A. M. Berlin, C. M. Malboeuf, E. M. Ryan, S. Gnerre, et al. 2012. Whole genome deep sequencing of HIV-1 reveals the impact of early minor variants upon immune recognition during acute infection. *PLoS Pathog.* 8: e1002529.
40. Read, E. L., A. A. Tovo-Dwyer, and A. K. Chakraborty. 2012. Stochastic effects are important in intrahost HIV evolution even when viral loads are high. *Proc. Natl. Acad. Sci. USA* 109: 19727–19732.
41. Kouyos, R. D., C. L. Althaus, and S. Bonhoeffer. 2006. Stochastic or deterministic: what is the effective population size of HIV-1? *Trends Microbiol.* 14: 507–511.